Journal of Biomechanics 79 (2018) 212–217

Contents lists available at ScienceDirect

Journal of Biomechanics

journal homepage: www.elsevier.com/locate/jbiomech
www.JBiomech.com

Short communication

Automated, accurate, and three-dimensional method for calculating sagittal slope of the tibial plateau

Mark J. Amirtharaj [a], Brendan M. Hardy [a], Robert N. Kent III [a], Danyal H. Nawabi [b], Thomas L. Wickiewicz [b], Andrew D. Pearle [b], Carl W. Imhauser [a,*]

[a] Department of Biomechanics, Hospital for Special Surgery, Weill Cornell Medicine of Cornell University, 535 E 70th St, New York, NY 10021, USA
[b] Department of Orthopedic Surgery, Hospital for Special Surgery, Weill Cornell Medicine of Cornell University, 535 E 70th St, New York, NY 10021, USA

ARTICLE INFO

Article history:
Accepted 31 July 2018

Keywords:
Algorithm
Tibia
Slope
Sagittal
Lateral plateau
Anterior cruciate ligament
Noncontact
Rupture

ABSTRACT

Increased posterior-inferior directed slope of the subchondral bone of the lateral tibial plateau is a risk factor for noncontact rupture of the anterior cruciate ligament (ACL). Previous measures of lateral tibial slope, however, vary from study to study and often lack documentation of their accuracy. These factors impede identifying the magnitude of lateral tibial slope that increases risk of noncontact ACL rupture. Therefore, we developed and evaluated a new method that (1) requires minimal user input; (2) employs 3D renderings of the tibia that are referenced to a 3D anatomic coordinate system; and (3) is precise, reliable, and accurate. The user first isolated the proximal tibia from computed tomography (CT) scans. Then, the algorithm placed the proximal tibia in an automatically generated tibial coordinate system. Next, it identified points along the rim of subchondral bone around the lateral tibial plateau, iteratively fit a plane to this rim of points, and, finally, referenced the plane to the tibial coordinate system. Precision and reliability of the lateral slope measurements were respectively assessed via standard deviation and intra- and inter-class correlation coefficients using CT scans of three cadaveric tibia. Accuracy was quantified by comparing changes in lateral tibial slope calculated by our algorithm to predefined *in silico* changes in slope. Precision, reliability, and accuracy were $\leq$0.18°, $\geq$0.998, and $\leq$0.13°, respectively. We will use our novel method to better understand the relationship between lateral tibial slope and knee biomechanics towards preventing ACL rupture and improving its treatment.

1. Introduction

Rupture of the anterior cruciate ligament (ACL) is a common, costly, and debilitating knee injury (Brophy et al., 2009; Griffin et al., 2006; Lohmander et al., 2007). Therefore, researchers have sought to identify factors that heighten risk for this lesion. One such factor is increased posterior-inferior directed slope of the lateral tibial plateau, which elevates risk of not only noncontact ACL rupture (Beynnon et al., 2014; Dare et al., 2015), but revision surgery (Ahmed et al., 2017), and instability in the setting of ACL deficiency (Rahnemai-Azar et al., 2017; Song et al., 2016).

Planar methods for measuring sagittal slope of the lateral tibial plateau yield variable results from study to study (Bisson and Gurske-DePerio, 2010; Wordeman et al., 2012), which impedes identifying the magnitude of tibial slope that increases risk of noncontact ACL rupture. Previous techniques have utilized lateral radiography or a single, sagittal slice from a magnetic resonance imaging (MRI) scan (Hashemi et al., 2010; Hudek et al., 2009). Although these two-dimensional (2D) methods are easy to implement, they have limitations. Specifically, sagittal slope of the medial and lateral compartments are difficult to distinguish on lateral radiographs (Hashemi et al., 2010; Hudek et al., 2009; Kessler et al., 2003). In addition, planar measures of slope using manually identified reference points exhibit variations ranging from ±1.4° to ±4.8° (Caylor et al., 2001; Hudek et al., 2009). Finally, inconsistent alignment of the tibia relative to the imaging device influences planar slope measurements by 3.1° to 14° (Kessler et al., 2003; Utzschneider et al., 2011).

Sagittal tibial slope has also been measured using 3D reconstructions of the proximal tibia from MRI. Simon et al. fit a plane to the medial and lateral subchondral surfaces of the tibial plateau including the tibial spine (Simon et al., 2010). Interestingly, the tibial spine exhibits high interpersonal variability (medial tibial spine volume measured 326 ± 171 mm^3 across 88 subjects), which may increase uncertainity of the slope measurement (Sturnick et al.,

* Corresponding author at: 535 E 70th St, New York, NY 10021, USA.
E-mail address: imhauserc@hss.edu (C.W. Imhauser).

https://doi.org/10.1016/j.jbiomech.2018.07.047
0021-9290/

2014). Amerinatanzi et al. calculated tibial slope from a 3D Gaussian curvature analysis that required extensive user input, which could be another source of variability (Amerinatanzi et al., 2017).

Identifying relationships between tibial slope and biomechanical function of the knee is important to understand why certain individuals are more susceptible to ACL rupture. Thus, we aimed to advance the ability to measure sagittal slope of the tibial plateau by describing and evaluating a method that (1) requires minimal user input; (2) uses 3D renderings of the tibia; and (3) is precise, reliable, and accurate.

2. Methods

2.1. Algorithm Description

The algorithm to quantify tibial slope consists of five steps: (1) generating a point cloud of the proximal tibia obtained from 3D image data; (2) defining an anatomic coordinate system for the proximal tibia; (3) identifying the lateral rim of the tibial plateau (RTP); (4) iteratively fitting a plane to the lateral RTP; and (5) computing the sagittal slope of the lateral RTP relative to the anatomic coordinate system. Steps two through five are automated via custom code developed using MATLAB (v2016b, Natick, MA).

(1) Generating the 3D tibial point cloud

Computed tomography (CT) scans (Biograph, Siemens Inc., Munich, Germany) of three cadaveric knee specimens free of joint degeneration, deformity, or injury were obtained (3 male; ages 21, 21, and 43). The specimens were all young and without injury, and, therefore, are representative of those suffering first-time, noncontact ACL rupture. Each specimen was scanned axially with 0.6 mm slice thickness and 0.5×0.5 mm^2 in-plane pixel dimensions (settings: 140 kV and 140 mA). Each tibia was segmented using grey value thresholding via Mimics software (Materialise Inc., Leuven, Belgium); then, the 3D spatial coordinates (or points) describing the tibial surface were exported in Stereolithography format (Fig. 1A). These data were subsequently imported into Geomagic software (3D Systems Inc., Rock Hill, SC), smoothed, and remeshed to a uniform point distribution (40% smoothing, 0.5 mm target edge length). Next, the tibial geometry was rotated to approximately align its long axis with the global Z-axis (Fig. 1B). Then, the proximal 15 cm of the tibia starting from the peak of the medial tibial spine was isolated, which corresponded to about 40% of the total length of the tibia (Fig. 1C). A tibial length of 15 cm is typically available in cadaver studies of knee joint biomechanics (Imhauser et al., 2013). This length also includes the tibial tubercle, whose geometry and location may vary from person to person (Brzobohatá et al., 2016). Finally, the rest of the tibial geometry was deleted and the proximal tibia was saved as an ASC vertex file.

(2) Defining the tibial coordinate system

The anatomical coordinate system for the proximal tibial geometry, or tibial coordinate system, was defined using a previously published method (Kai et al., 2014). First, the long axis (Z-axis) was computed via principle component analysis (PCA) (Fig. 2A). PCA identified the direction of most variance in the point data describing the proximal tibia (Pearson, 1901); this direction aligned with the tibial long axis. Next, the medial-lateral (ML) and anterior-posterior (AP) axes of the tibial coordinate system were defined using the most contoured ellipse, which has the largest sum of major and minor axes lengths (Fig. 2B, C). The most contoured ellipse was identified by successively fitting an ellipse to point data located within transverse slices perpendicular to the long axis of the tibia in 0.3 mm increments. The major and minor axes of the most contoured ellipse were set as the respective ML (Y-axis) and AP (X-axis) axes of the tibial coordinate system (Fig. 2C, D) (Bobrowitsch et al., 2007); the center of this ellipse was defined as the origin of the tibial coordinate system.

(3) Identifying the lateral rim of the tibial plateau

The lateral tibial plateau was isolated by eliminating all points >20 mm inferior and >10 mm medial to the peak of the medial tibial spine. This range isolated the set of points describing the surface of the lateral plateau and a portion of the proximal tibial metaphysis. Then, this set of points was used to identify the periphery, or rim, of the lateral plateau. Specifically, the points on the lateral RTP were defined to correspond to the location of maximum curvature when traversing radially over the edge of the tibia and inferiorly down the tibial metaphysis (Fig. 3). To identify the points comprising the lateral RTP, first, a point located centrally on the lateral plateau provided a reference for our algorithm. This central point was specified to be at the peak of the medial tibial spine in the AP direction, 25% of the length of the major axis of the most contoured ellipse in the ML direction, and at the origin of the anatomic coordinate system in the superior-inferior (SI) direction (Fig. 3). These

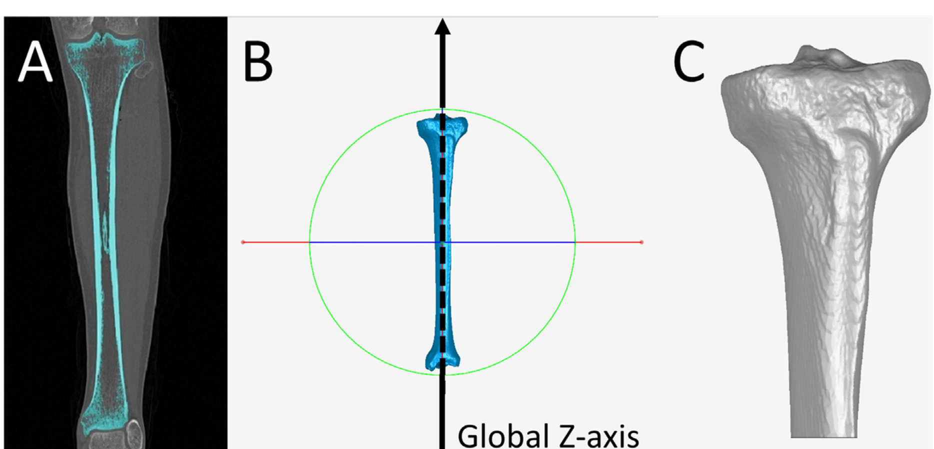

Fig. 1. Overview of the steps used to generate the point cloud describing the proximal tibial geometry. The steps were (A) masking each 2D slice of the tibial geometry from a CT scan as outlined in blue and then developing a 3D rendering; (B) approximately aligning the long axis of the 3D tibial geometry with the global Z-axis; and (C) isolating the proximal 15 cm of the tibial geometry. (For interpretation of the references to colour in this figure legend, the reader is referred to the web version of this article.)